3D Assessments For Design And Performance Analysis Of Uo_2 Pellets

A.C. Marino, G.L. Demarco & P.C. Florido

División Diseños Avanzados y Evaluación Económica - DAEE
Centro Atómico Bariloche - CAB
Comisión Nacional de Energía Atómica - CNEA
R8402AGP Bariloche
Argentina
e-mail: marino@cab.cnea.gov.ar

ABSTRACT

The geometry of a fuel pellet is a compromise among the intention to maximize UO_2 content and minimize the temperature profile taking into account the thermo-mechanical behavior, the economy and the safety of the fuel management during and after irradiation. “Dishings”, “shoulders”, “chamfers” and/or “a central hole” on a cylinder with an improved *l/d* relation (length of the pellet / diameter) are introduced in order to optimize the shape of the pellet. The coupling of the BACO code and the MECOM tools constitutes a complete system for the 3D analysis of the stress-strain state of the pellet under irradiation. CANDU and PHWR MOX fuel will be used to illustrate the qualitative agreement between experimental data and calculations.

1. INTRODUCTION

A fuel element is a set of fuel rods assembled with structural components like “grids” and “spacers”. Each fuel rod is a Zircaloy-made tube (or “cladding”) filled with UO_2 pellets. The geometry of the fuel pellet has symmetry of revolution taking into account the thermo-mechanical behavior during irradiation at the nuclear power plant.

The starting point for the design of an UO_2 pellet is a simple cylinder. However, that shape for a pellet under irradiation leads to a “bamboo” way for the fuel rod due to the temperature profile. The *l/d* relation (length of the pellet / diameter) is optimized in order to minimize that geometric behavior. A few modifications in the cylinder are introduced in order to reduce the pellet to pellet axial stresses and the PCMI (Pellet-Cladding Mechanical Interaction) in particular at the top and at the bottom of the cylinder. Those stresses are reduced by using “dishings”, “shoulders” and “chamfers” in the cylinder. In fact, we reduce stresses by sectioning the parts of the pellet where the maximum deformations are present. Then it becomes an optimized UO_2 pellet. The support of that designs is made with the irradiation of normal and unusual pellet shapes. The study of conics, flat and/or hollow pellets under irradiation were presented in several papers plus the study of the relative influence of the variation of *l/d* and the size of dishing, chamfer

and shoulder. We intent to maximize the UO_2 content and minimize the temperature profile, reduce the effect o PCMI (Pellet-Cladding Mechanical Interaction) and PCI-SCC (Pellet Cladding Interaction - Stress Corrosion Cracking) taking into account the economy and the safety of the fuel management during and after irradiation.

Diameter gauge measurements have revealed the presence of increased dimensions at the position of pellet ends during and after power ramps resulting from the wheatsheaf of hourglass or bamboo shape adopted by the pellets. A detailed diameter measurement reveals the presence of a secondary ridge at the middle of the pellet [1]. The change is on account of the poor thermal conductivity of the UO_2 fuel and the consequent differential thermal expansion caused by the temperature difference between the interior and exterior of the pellets. A good example of the diameter change during power ramp at the pellets will be presented bellow. Ridge formation to a greater or lesser extent is found in all small gap rods when power ramped. The axial displacement of the pellets and the changing in the axial power profile of the long fuels as PWR and BWR could lead to the formation of ridges at different heights of the rod (ratcheting). The small length of CANDU and experimental fuel rods guaranties a good positioning of pellet ends with the ridge due to the absence of ratcheting. We could expect the presence of clear ridges in these types of fuels when the gap is closed for power ramping, swelling, creep-down or a combination of them. This particular situation is the usual condition under irradiation for the CANDU fuel rods where the cladding is collapsible and no gap is present.

The thermo-mechanical behavior of a nuclear fuel rod under irradiation is a complex process where too many coupled physics and chemical phenomena are present. The BACO code (BArra COmbustible, Spanish expression for “fuel rod”) was developed at the Atomic Energy National Commission of Argentina (CNEA, “Comisión Nacional de Energía Atómica”) for the simulation of the behavior of nuclear fuel rods under irradiation. We are using a quasi-two-dimensional approach and with its use several 3D (three dimensional) topics as the stress-strain state can be explained. Nevertheless, we enhance the BACO code results by using “ad hoc” tools based on a finite elements scheme developed at the MECOM and DAEE Divisions (Bariloche Atomic Center, CNEA). The temperature profile and the boundary conditions, among others, are calculated with BACO to be inserted as input data in the MECOM tools. Then we calculate the 3D stress-strain state and the deformations of the UO_2 pellet. The MECOM tools include the same laws for elasticity and thermal expansion than the BACO code. We find the shape of the pellet under irradiation showing the stress profiles, the bamboo effect and others 3D effects as the presence of the secondary ridge and the radial profile of a fuel rod.

In this paper we will show the symbiosis between BACO and MECOM tools by using CANDU, and PHWR MOX fuels as input data. The results will show the good agreement between experimental data and calculations particularly for the radial profile of pellet after irradiation. The coupling of BACO and MECOM tools constitutes a powerful system for the analysis and design of nuclear fuel pellets taking into account the best

combination of *l/d* and the dimensioning of dishing, shoulder and chamfers. Innovative or unusual pellet shapes can be analyzed by using these “ad hoc” tools against the actual tendency to use commercial software adapted for nuclear applications.

2. THE BACO CODE

2.1. BACO code description

The BACO code structure and models have already been described in the reference [2], including steady state and transient thermal analysis. Nowadays, the number of instructions is about twelve thousand FORTRAN 90 lines. Data post-processing and the coupling with 3D calculation using finite elements improve the output of BACO and the analysis of results.

On modeling the UO_2 pellet, elastic deformation, thermal expansion, creep, swelling, densification, restructuring, cracks and fission gas release are included. While for the Zry cladding, the code models elastic deformation, thermal expansion, anisotropic plastic deformation, and creep and growth under irradiation. The modular structure of the code easily allows the adding of different material properties. It can be used for any geometrical dimensions of cylindrical fuel rods with UO_2 pellets (either compact or hollow, with or without dishing) and Zry cladding.

A special feature of the BACO code is to include a complete treatment of the fuel with or without mechanical contact of the pellet surface and the clad, in any irradiation stage, and then could be fully used to model self standing clad sheets (like LWR and Atucha fuel rods) [3] or collapsible clad sheets (like CANDU and Embalse fuel rods) [4], without special changes in the physical models triggered by the user input.

Fuel rod power history and either cladding or coolant outside temperatures must be given to the program. Rod performance is numerically simulated using finite time steps (finite differential scheme). The code automatically selects time steps according to physical criteria. Temperature profiles within pellet and cladding, main stresses at pellet and cladding, radial and axial crack pattern in the pellet, main strains and hot geometry of pellet and cladding, change in porosity, grain size and restructuring of the pellet, fission gas release to the free volume in the rod, trapped gas distribution in the fuel and in the UO_2 grain boundary, internal gas pressure and current composition of the internal gas, dishing shape evolution, are calculated. The output of the code contains the distribution along the rod axis of these variables.

2.2. Numerical treatment

Summary of assumptions taking into account the numerical treatment:

- Cylindrical symmetry.
- Pellet and clad are divided into circular concentric rings.

- For the numerical modeling the hypothesis of axial symmetry and modified plane strain (constant axial strain) is adopted. The three-dimensional stress-strain problem is reduced to a quasi-two-dimensional problem.
- Behavior equations integrated with a finite difference scheme.
- Fuel pin irradiation life is divided into subsequent finite time steps for the temporal integration.

2.3. Mechanical treatment

It is assumed that during the time interval (t_0, $t_0 + \delta t$), the strain-stress increments can be expressed as the superposition of the strain-stress increments due to the different existing deformation mechanisms. Defining the strain-stress state at time t_0 and at the corresponding time $t_0 + \delta t$ (with δt very small), it is possible to calculate as follows:

$$\dot{\varepsilon} = \varepsilon_0 + \delta\varepsilon$$

where:

ε_0 : is a stress-strain magnitude at t_0, and
$\delta\varepsilon$: is the corresponding time step variation.

The equations to be integrated are, essentially, the compatibility equation of each ring, the equilibrium equation, and the Hook's generalized equations, subject to the appropriate boundary conditions. That means a system of seven coupled differential equations. The finite differences approximation lead to a non-linear system of algebraic equations, which is linearised through a Taylor expansion. The previously described system for a given time increment can be solved for the main stresses by direct matrix inversion.

2.4. Thermal treatment

The temperature distribution in the pellet or cladding for the strain state results from solving Fourier equation for steady state heat transmission. The boundary condition is a fixed temperature at the cladding external surface and we know the heat generated.

The details of the mechanical and thermal treatment and the pellet, cladding and constitutive equations are available in the reference [2].

3. MECOM TOOLS

The 3D finite element (FEM) calculations were performed with a set of tools developed at the Computational Mechanics (MeCom) Division at the Bariloche Atomic Center (CAB), CNEA. Basically, these are grouped in to software packages, “acdp95” [5] and “gpfep99” [6], kindly made available to us by its main developers.

The package acdp95 includes tools for mesh generation and optimization [7] and a complete collection of visualization programs. Non structured meshes composed of tetrahedral elements for arbitrary geometries can be obtained. Visualization tools for viewing meshes and the FEM solutions over these meshes (scalar and vectorial) are available.

The package “gpfep99” is the FEM solver. In fact, it is a system to generate FEM solvers. It is distributed in source form (written in FORTRAN 77). It is possible for the user to write a subroutine to modify the code. In our case, we wrote no more than three hundred lines of code (100 for the elasticity problem, 100 for the stress calculation and 100 for the Von Misses stress calculation). “gpfep99” can handle time dependent and non linear problems and there are several types of elements (not only linear tetrahedral) implemented. There is also a paralellizable version [8]. The solutions obtained with “gpfep99” can be visualized with the “acdp95” tools.

4. BACO + MECOM

A first approximation of the fuel rod behavior is made by using the BACO code. The treatment is quasi-bidimensional at this stage but using the complete set of models an options of BACO mentioned above. We generate the input data for the MeCom Tools, in particular the geometry of the pellets and the boundary conditions for a particular time of the irradiation. The geometry of the pellet includes the dishing evolution [9], the shoulders and the deformations calculated by BACO. The main boundary conditions are the temperature profile and the gas pressure. Porosity, crack pattern and thermal conductivity can be included into MeCom for a best estimation of its thermal behavior. The result is the new 3D geometry of the pellets and the 3D maps of stresses and strains. At present we are just including elasticity and thermal expansion into the FEM solver. It is not included a way for stress release like creep, cracks opening and/or plasticity. The stress-strain state results in an extreme condition of behavior with the highest stress in the pellet more than the most demanding condition. BACO runs and is developed under a Windows environment by using Digital FORTRAN and/or Lahey FORTRAN compilers. MeCom tools runs under LINUX operative system. “Cygwin” makes the coupling of them. “Cygwin” is a Linux-like environment for Windows. Then, we do not need to change the system to use both sets of codes.

5. A 3D CANDU FUEL PELLET SIMULATION APPROACH

We analyze the 3D behavior of a normal CANDU fuel pellet without chamfers for illustrative purposes. We use the temperature profile of the figure 1 and other parameters calculated with BACO for a CANDU fuel during high demanding conditions of operation. The mesh for finite elements calculation with MeCom is included in the figure 3. We are using more than 15000 finite elements of volume. The von Misses stresses are included in the figure 3 where three different views facilitate the analysis. The stress state obtained shows high values for stress due to the absence of a

mechanism to relax them, as crack opening and/or creep. The highest stresses are located at the shoulders of the pellet where more cracks are usually present.

The figure 4 presents the radial deformations of the CANDU pellet. Here, the highest deformations are presented in the area of shoulders where the ridges are usually present. The figure 4 includes a plot with the radial profile of the pellet. The way of that plot follows the way of the experimental radial profile of CANDU fuels. We assume that the cladding profile is the same than the pellet profile. This is a strong assumption but it is sustained for the collapsibility of the CANDU fuels. The height of the ridges has a smaller value than the ones reported in the literature but it kept a high qualitative value [10]. Finally, we draw the 3D pellet of the figure 2 by using the previous calculation.

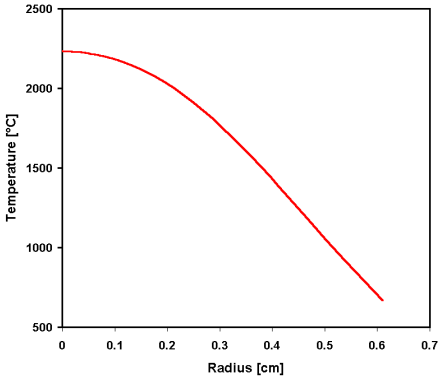

FIGURE 1: CANDU PELLET TEMPERATURE PROFILE.

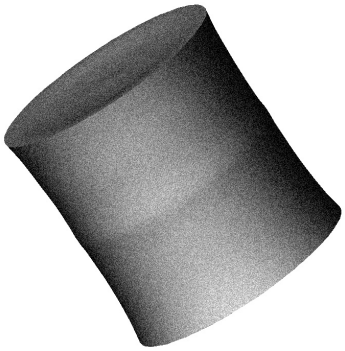

FIGURE 2: 3D CANDU PELLET CALCULATED WITH BACO + MECOM TOOLS. RADIAL DEFORMATIONS ARE EMPHASIZED.

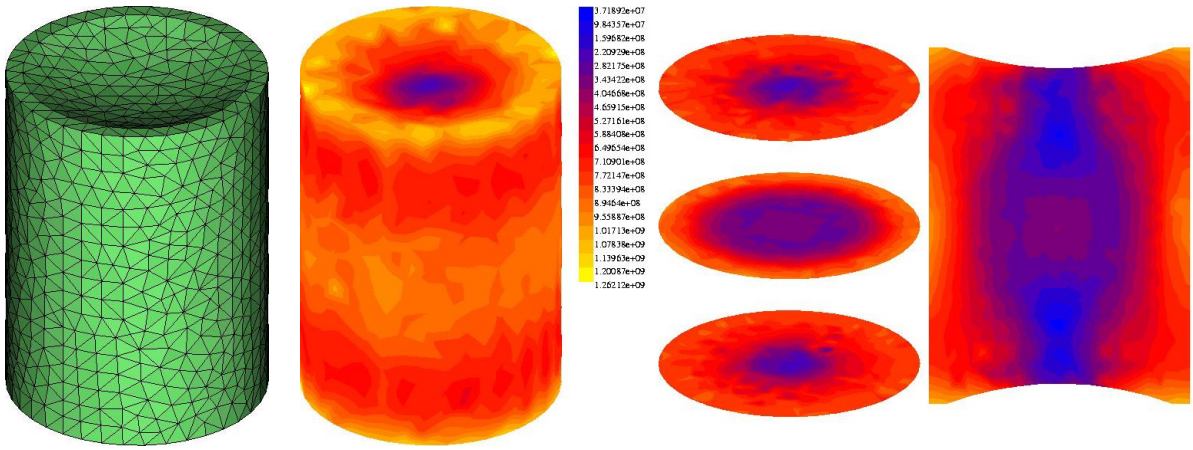

FIGURE 3: MESH AND VON MISES EQUIVALENT STRESS OF THE PELLET.

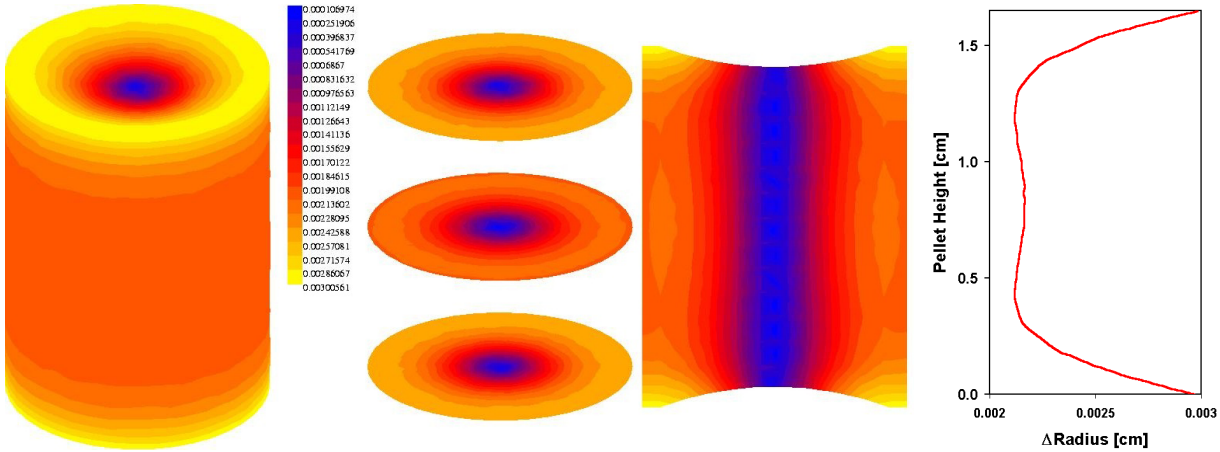

FIGURE 4: RADIAL DEFORMATIONS IN A CANDU FUEL PELLET.

6. PHWR MOX EXPERIMENTAL SUPPORT

The irradiation of the first prototypes of PHWR MOX fuels fabricated in Argentina began in 1986. These experiments were made in the HFR-Petten reactor, Holland. The six rods were fabricated in the α Facility (CNEA, Argentina) [11, 12 and 13]. This set of irradiations is included in the IFPE of the OECD [17]. We use one of those irradiations as experimental support of the codes. An irradiation of PHWR extended burnup was performed with the MOX fuel rod named A.1.3. The burnup of extraction was 15000 MWd/tonUO_2, three times the usual burnup at end of life of a PHWR NPP, including a demanding power ramp at EOL (End Of Life). The radial power profile during the base irradiation, before the power ramp, presented a maximum value at the bottom of the fuel rod. The temperature profile calculated with the BACO code is sketched at the figure 5. The maximum value of temperature was achieved at the bottom of the rod. The power ramp was performed at the Pool Side Facility of the HFR-Petten Reactor. We flip the position of the MOX fuel then, the maximum value of power and temperature were done in the opposite side of the rod. This situation produced a strong power ramp of ~300 W/cm in one of the extremities of the rod. The new temperature profile is included in the figure 6.

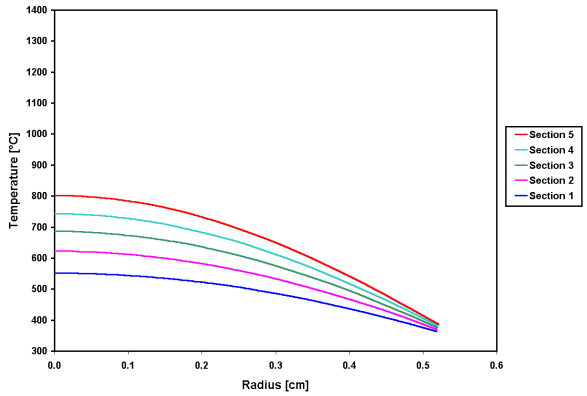

FIGURE 5: TEMPERATURE PROFILE OF THE MOX FUEL A.1.3 BEFORE RAMPING AT EOL (SECTION 1 AT THE BOTTOM OF THE FUEL ROD).

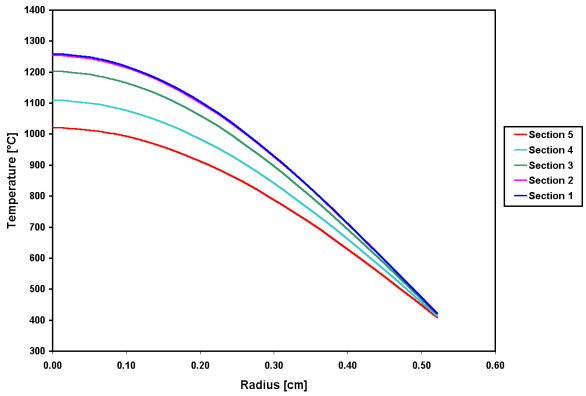

FIGURE 6: TEMPERATURE PROFILE OF THE MOX FUEL A.1.3 AT THE TOP POWER RAMP AT EOL (SECTION 1 AT THE TOP OF THE FUEL ROD).

We calculate the stress-strain state of the MOX fuel rod before and after the final ramp by using the previous temperature profile and the calculated inner pressure as boundary conditions and pellet data, among others. The radial deformations of the pellets are included in the figures 7 and 8. Here we observe the “bamboo” effect and the presence of a small secondary ridge as we expected in the 5 sections of the rod.

The figure 9 includes the fuel rod profile of the MOX rod after the power ramp and the representation of the stack of pellets. It is a strong assumption to correlate the experimental deformations of the MOX fuel with the pellets profile calculated with BACO + MeCom. Nevertheless, there is a strong correlation from a qualitative point of view and the clad wall thickness had only a small effect on the ridge height as was experimentally observed [14].

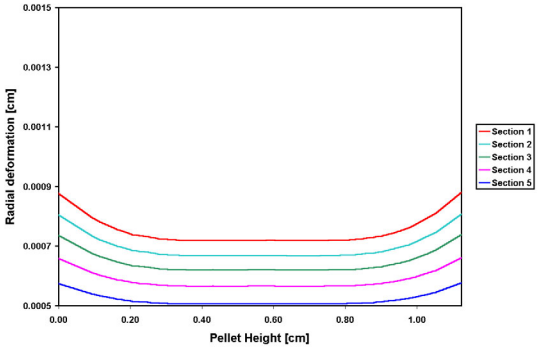

FIGURE 7: PELLET PROFILE OF FIVE AXIAL SECTIONS OF THE MOX FUEL A.1.3 BEFORE RAMPING AT EOL.

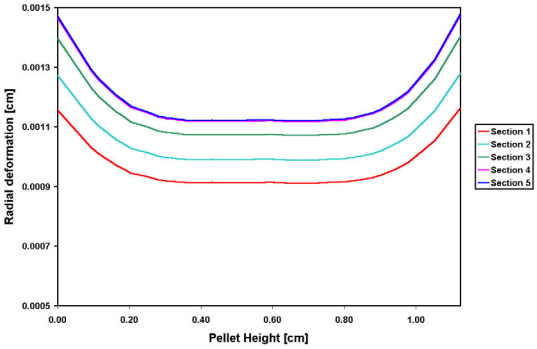

FIGURE 8: PELLET PROFILE OF THE FIVE AXIAL SECTIONS OF THE MOX FUEL A.1.3 AT THE TOP POWER RAMP AT EOL.

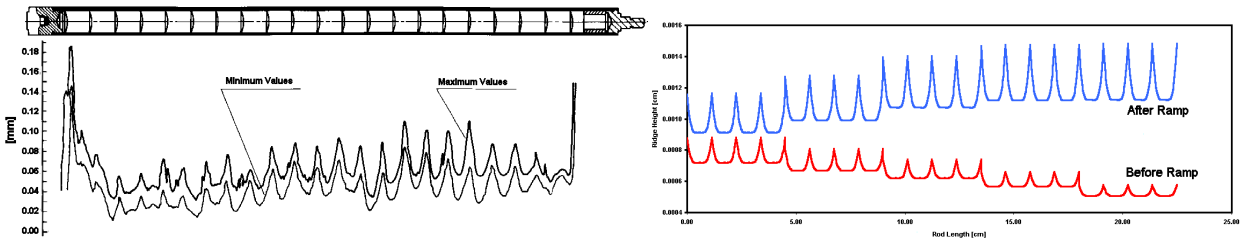

FIGURE 9: FUEL ROD PROFILE OF THE MOX FUEL A.1.3 BEFORE AND AFTER THE POWER RAMP. EXPERIMENTAL (TOP CURVES) AND CALCULATED (LOWER CURVES) VALUES.

7. CANDU FUEL EXPERIMENTAL SUPPORT

At this point we will analyze several fuel pellets with real and/or unusual geometric shapes. The pellet of figure 3 will be used in this analysis and it will be named (a) “normal” pellet, a CANDU fuel pellet with a shoulder and without “chamfers”. The figure 10 includes the following pellets: (b) a flat pellet without dishing, (c) a hollowed pellet without dishing, (d) a standard CANDU fuel pellet, (e) a conic pellet with a dish at the top, and (f) a “barrel” (double conic pellet) with one dish. We include the radial deformation as the difference between the present radius and the original one for each pellet.

The radial pellet profile of the pellet with the dishing (see pellet (a) of figure 3) presents more deformation than the “flat” pellet without dishing (see pellet (b) of figure 10). This agrees with experimental evidence included in reference [15].

The presence of “chamfers” in the pellet (see the standard CANDU pellet (d) of figure 10) disables the presence of the zone of the pellet with the highest deformation. In fact, the chamfers reduce the radial deformation along the entire pellet as we expect by design.

The presence of a central hollow in the pellet (see pellet (c) of the figure 10) reduces the bamboo shape and the radial deformation along the pellet.

The most radical pellets as the (e) and (f) of figure 10 reduce the ridging but there is a no contact situation at the extreme position of the conic sections of the pellet. These pellets reduce the content of UO_2 and they do not keep the concept of a collapsible cladding for CANDU fuels.

These observations among others agree with the experimental observations [10,16].

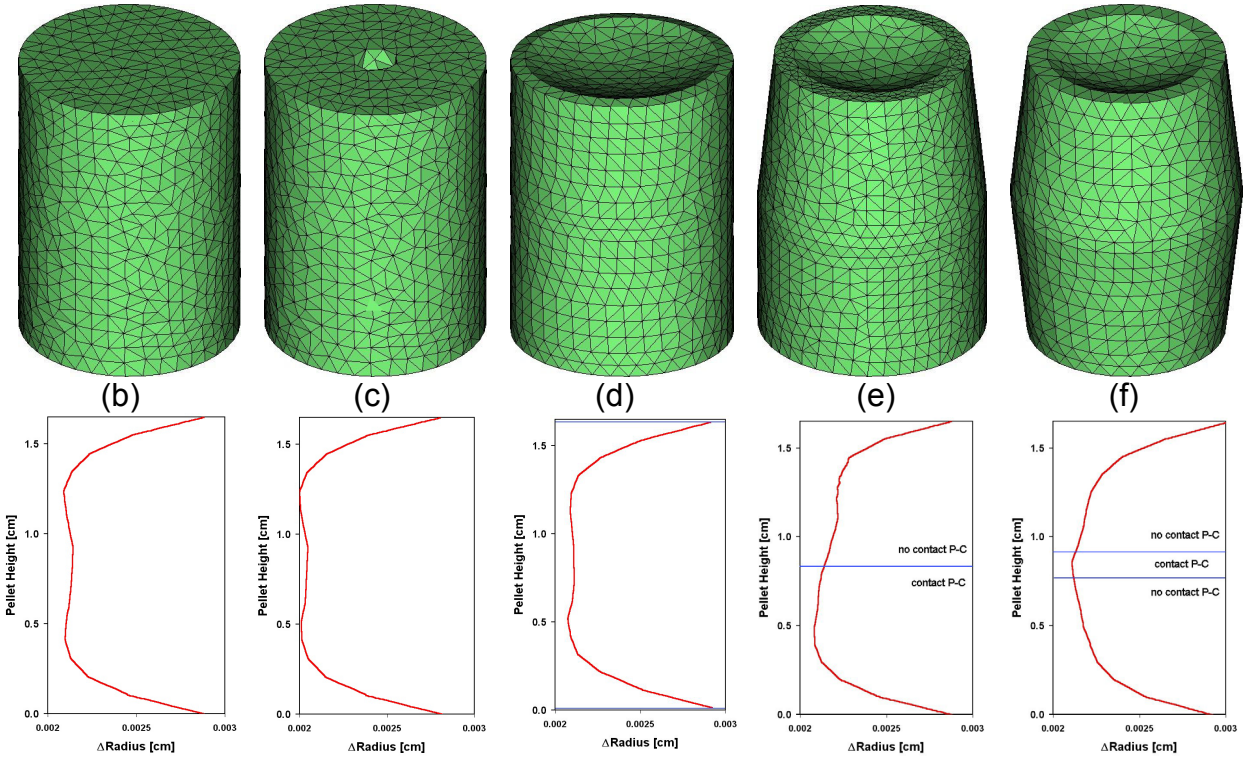

FIGURE 10: THE MESHES OF EXPERIMENTAL CANDU FUEL PELLETS OF REF [10]. AND THEIR RADIAL DEFORMATIONS. ΔR IS THE DIFERENCE BETWEEN THE PRESENT RADIUS AND THE ORIGINAL ONE.

8. AN APPROACH TO A 3D PELLET CRACKS SIMULATION

An approach to a cracked pellet analysis can be initiated with the two cracks defined in the figure 11: (a) a single crack at the top of the pellet, and (b) a single crack crossing from the top to the bottom of the pellet. The radial profile of the single cracked pellet (a) shows a maximum value of the radial deformation close to the crack. The minimum deformation is present in the opposite side of the crack (see figure 11). The case of a full crack (b) presents the maximum deformation close to the cracks but, the minimum value is located at $\pm 30°$ of the crack. These curves of minimum values for the radial deformations looks equivalents in both types of cracked pellets. The maximum value of the deformation reaches the same value for both type of cracked pellets. However, the pellet type (a) presents that maximum at the top and there is a strong decrement of its deformation along the height of the pellet. On the other side, the pellet type (b) keeps the maxim value along the heights of the pellet and both curves of deformation looks very similar with an increment of the secondary ridge close to the middle of its large crack. It is clearly shown that the presence of the “real” cracks type (a) increases the ridging at its location but it reduces the deformation along the rest of the pellet. This point of view is in agreement with the previous radial profiles calculated for different type of pellets without the presence of cracks where the ridges were underestimated.

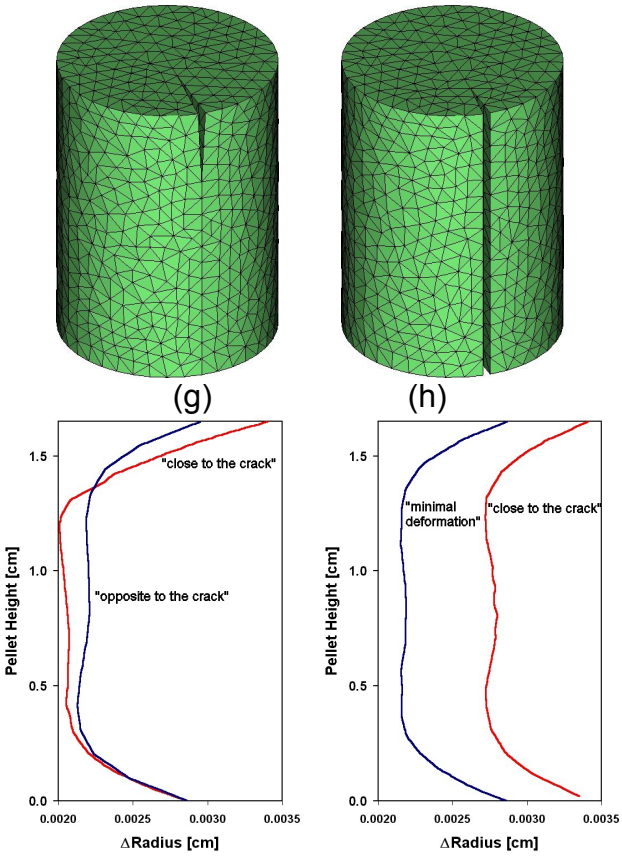

FIGURE 11: TWO TYPE OF CRACKED FUEL FOR STRESS ANALYSIS AND ITS RADIAL PROFILE.

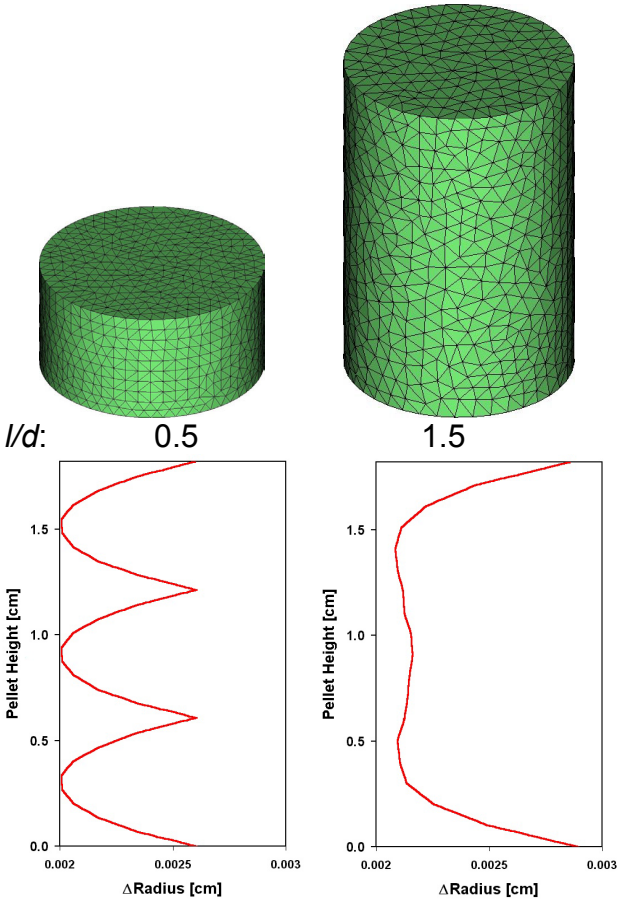

FIGURE 12: MESHES OF CANDU PELLETS FOR THE “l/d” ANALYSIS.

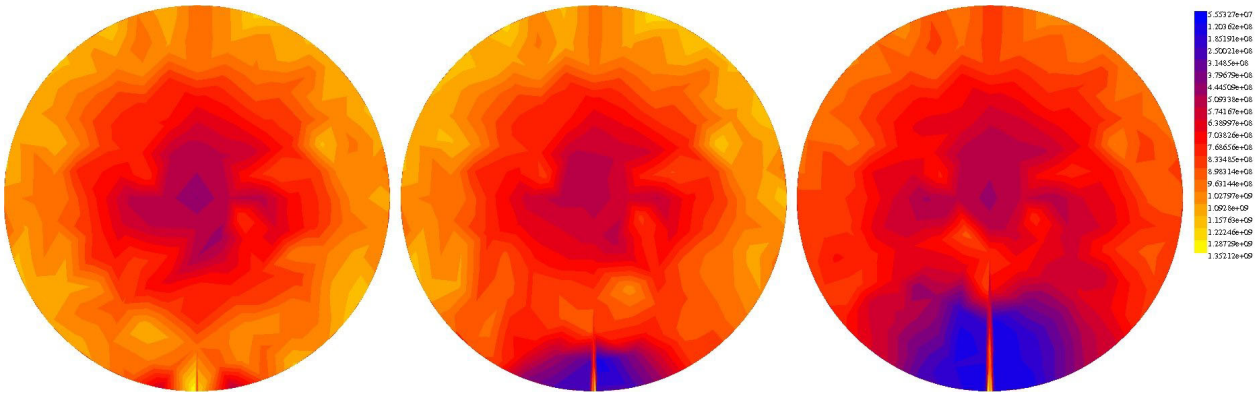

FIGURE 13: TOP VIEW OF THE VON MISSES EQUIVALENT STRESS FOR THREE CRACKED PELLETS TYPE (a) WITH DIFFERENTS VALUES OF PENETRATION.

The figure 13 shows the von Misses equivalent stress for three cracked pellets type (a) with three values of penetration. We observe a concentration of stresses at the vertex of the cracks. It is clearly shown an effect of stress release due to the presence of

the crack. This analysis could be continued with the inclusion of several cracks in the pellet in order to reduce stresses. The inclusion of these cracks in the previous shapes could to induce to lose the qualitative purpose of the present analysis.

9. PELLET DESIGN

We mentioned above that the optimization of a fuel pellet geometry could be approached with the finding of the best *l/d* relation. It is confirmed by the agreement with several experiments present in the literature [10, 16]. The figure 12 includes two types of pellets with *l/d* = 0.5 (a) and *l/d* = 1.5 (b). We could find that the ridging is reduced when *l/d* is reduced with a perfect agreement with experimental observation. The curve of figure 14 includes the experimental values and our calculations with different *l/d* values. There is not a clear correlation between experimental results and BACO calculations because the experimental evaluation of the fuel ridging was not clearly explained in the measurements performed in the references, however for a qualitative purpose we see that the global trends of the measurements of the mean ridge height are the same than the radial deformations of the pellets. We extend the qualitative agreement by varying shoulders and chamfers as it is shown in figure 14. The increment of *l/d* over more than 1.3 produces the maximum value of deformation. The decrement of *l/*d produces a convergence to the lowest values for the radial deformation. These trends are present in all the BACO calculations.

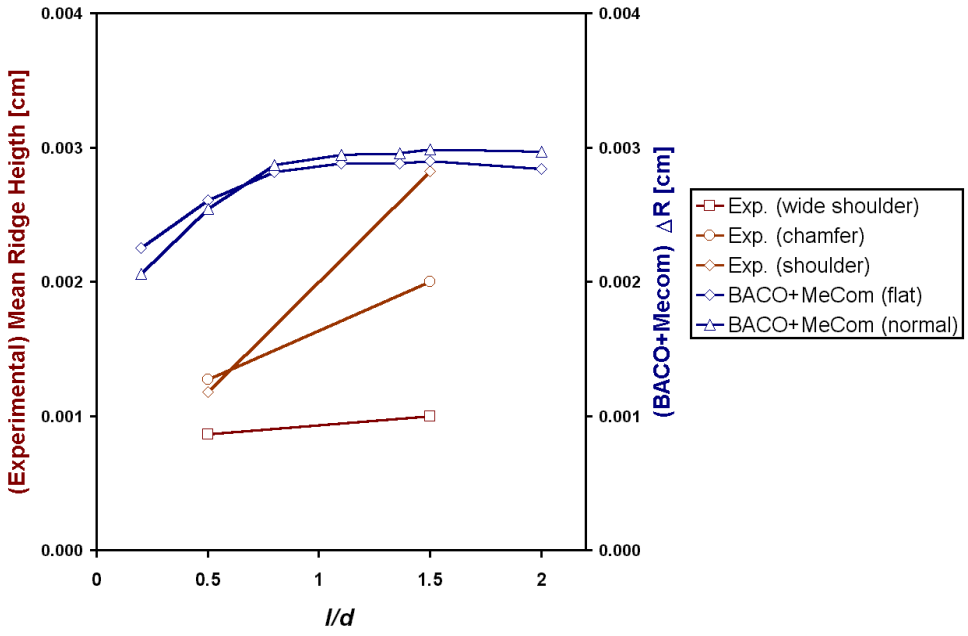

FIGURE 14: CORRELATION BETWEEN EXPERIMENTAL MEAN RIDGE HEIGHT AND RADIAL DEFORMATION (∆R) CALCULATED BY VARYING THE l/d RELATION.

10. CONCLUSIONS

We presented the symbiosis between BACO and MECOM tools by using CANDU, CARA, and PHWR MOX fuels as input data. At present, we are including elasticity in the 3D evaluation and all the set of modeling of BACO, however the results show a good agreement between experimental data and calculations particularly for the radial profile of pellet after irradiation. The coupling of BACO and MECOM tools constitutes a powerful system for the analysis and design of nuclear fuel pellets taking into account very different shapes of the fuel pellets, the best combination of *l/d* and the dimensioning of dishing, shoulder and chamfers. The influence of the cracks was established appointed as a way to increase ridging and to release stresses. We mention: a) the reduction of the deformation of hollowed pellet, b) the absence of ridging where conic shapes are used for the pellets, c) the increment of ridging when a dishing is present in the pellet, d) the reduction of ridging due to chamfers, and e) the trends of radial deformation by the variation of *l/d*, as interesting examples by using BACO + MeCom. Innovative or unusual pellet shapes can be analyzed by using these “ad hoc” tools against the actual tendency to use commercial software adapted for nuclear applications. We emphasize the economical aspect of these tools where a few running of the codes can reduce the number of experimental irradiations in an expensive programme and it provides a frame for the analysis of the experiments.

ACKNOWLEDGMENTS

Dr. E. Dari and Dr. G. Buscaglia who kindly made available to us the MeCom tools.
Dr. H. Troiani who carefully read the paper and several suggestions.

REFERENCES

1. BENTEJAC F. & HOURDEQUIN N., “TOUTATIS, an Application of the Cast3M Finite Element Code Three-dimensional Modelling”, “Les Journées de Cadarache 2004: International Seminar on Pellet-Clad Interaction in Water Reactor Fuels (PCI-2004)” organized by CEA Cadarache/DEN/DEC In co-operation with OECD/NEA, IAEA, EDF, FRAMATONE ANP, COGEMA, 9 to 11 of March 2004, Aix en Provence, France.
2. MARINO A. C., SAVINO E. J. & HARRIAGUE S., “BACO (BArra COmbustible) Code Version 2.20: a thermo-mechanical description of a nuclear fuel rod”, J. Nuc. Mat. Vol. 229, April II, 1996 (p155-168).
3. MARINO A. C. & SAVINO E. J., “Sensitivity analysis applied to nuclear fuel performance related to fabrication parameters and experiments“, 14th International Conference on Structural Mechanics in Reactor Technology, Paper C01/7, SMiRT 14, August 17-22, 1997, Lyon, France.
4. MARINO A. C., “Computer simulation of the behaviour and performance of a CANDU fuel rod.”, 5th International Conference on CANDU fuel, 1997, September 21-24, Toronto, Ontario, Canada.
5. DE OLIVEIRA M. et. al., "An Object Oriented Tool for Automatic Surface Mesh

Generation using the Advancing Front Technique", Latin American Applied Research 27 pp.39-49 (1997).

6. BUSCAGLIA G. et. al., "Un programa general de elementos finitos en paralelo", 6to. Congreso Argentino de Mecánica Computacional, MECOM'99, Mendoza, Argentina, Sep. 1999.
7. ZAVATTIERI P., BUSCAGLIA G., and DARI E., "Finite element mesh optimization in three dimensions" , Latin American Applied Research, 26 pp. 233-236 (1996).
8. DARI E. et. al, "A Parallel General Purpose Finite Element System", IX SIAM Conference on Parallel Processing for Scientific Computing, San Antonio, Texas, USA, March 1999.
9. MARINO A. C., “Crack and dishing evolution models and PCI-SCC considerations for fuel pellets in a quasi-bidimensional environment”, “Les Journées de Cadarache 2004: International Seminar on Pellet-Clad Interaction in Water Reactor Fuels (PCI-2004)” organized by CEA Cadarache/DEN/DEC In co-operation with OECD/NEA, IAEA, EDF, FRAMATONE ANP, CO4GEMA, 9 to 11 of March 2004, Aix en Provence, France.
10. HASTINGS I. J., CARTER T. J., DA SILVA R., FEHRENBACH P. J., HARDY D. G. and WOOD J. C., “CANDU fuel performance: Influence of fabrication variables”, IAEA-CNEA International Seminar on Heavy Water Reactor Fuel Technology, S. C. de Bariloche (1983), AECL MISC 250 (1983).
11. MARINO A. C., PÉREZ E. E. & ADELFANG P., “Argentine Nuclear Fuels MOX irradiated in the Petten Reactor, Experience analysis with the BACO code”, IAEA Technical Committee Meeting on Water Reactor Fuel Element Modeling at High Burnup and Its Experimental Support. Windermere, United Kingdom, September, 1994, IAEA-TECDOC-957.
12. MARINO A. C., PÉREZ E. E. & ADELFANG P., “Irradiation of Argentine MOX fuels. Post-irradiation results and analysis.”, IAEA Technical Committee Meeting on Recycling of Plutonium and Uranium in Water Reactor Fuel. Newby Bridge, Windermere, United Kingdom, 3-7 July 1995, IAEA-TECDOC-941.
13. MARINO A. C., PÉREZ E. E. & ADELFANG P., “Irradiation of Argentine MOX fuels. Post-irradiation results and experimental analysis with the BACO code.”, Journal of Nuclear Materials Vol. 229, April II, 1996 (p169-186).
14. GRAZIANI U., “Experimental Data Following an 85 % Increase of the IFA-509 Assembly Power at 3800 MWd/tUO_2”, HPR-229 EHPG Hankø, Norway, 17th – 21st June 1979.
15. KOLSTAD E. et al., “Review of Test Results on Gap Closure Behaviour and Mechanical Interaction Effects in the HBWR”, HWR-89 May 1983.
16. CARTER, T. J., “Experimental Investigation of Various Pellet Geometries to Reduce Strains in Zirconium Alloy Cladding”, Nuclear Technology 45 (1979) 166-176.
17. Turnbull J. A., J. C. Killeen & E. Sartori, “Experimental Data on PCI and PCMI within the IFPE Database”, “Les Journées de Cadarache 2004: International Seminar on Pellet-Clad Interaction in Water Reactor Fuels (PCI-2004)” organized

by CEA Cadarache/DEN/DEC In co-operation with OECD/NEA, IAEA, EDF, FRAMATONE ANP, CO4GEMA, 9 to 11 of March 2004, Aix en Provence, France.